Characteristic X-Ray Production in Single Crystals (Al, Cu) by Proton Bombardment. I. Protons of 70 to 100 keV*

J. M. KHAN, D. L. POTTER, AND R. D. WORLEY
University of California, Lawrence Radiation Laboratory, Livermore, California
AND
HAROLD P. SMITH, JR.
University of California, Berkeley, California

(Received 25 March 1966)

Characteristic x rays have been observed from single crystals of aluminum (K shell) and copper (L shell) during bombardment by 70- to 100-keV protons. The thick-target yield was found to be sensitive to the orientation of the crystals. Studies have been performed in the region of the [011] direction (at 45° to the crystal surface normal) and across the (100) plane at 30° to the normal. A yield contour at the [011] direction is presented over an angular region of 20°×20° and is compared with a polycrystalline value. A single-crystal yield exceeded the polycrystalline value by as much as 30% at one point. For copper the largest observed maximum-to-minimum yield ratio in the vicinity of the [011] direction was 15 to 1. The effect of surface contamination has been measured for selected sweeps. Also included is a calculation of a proton-crystal potential and comparison with a planar-averaged Nielsen potential.

INTRODUCTION

DURING ion bombardment of a monocrystalline solid, various phenomena were measured which demonstrated the importance of considering the crystallographic orientation of the target with respect to the ion beam. In particular, if the ion beam is parallel to certain crystallographic directions, significant changes occur in the measured ion penetration range,[1–4] sputtering yield coefficient,[5,6] ion transmission through or reflection from the target crystal,[7,8] and nuclear-reaction[9] and characteristic x-ray yield.[10] In the last category Brandt *et al.*[10] observed a factor of 2 decrease in the characteristic x-ray yield in aluminum and copper with the proton beam parallel to the [011] direction. It was noted that the full width at half-maximum of this yield curve decreased from 6.7° to 5.7° when the proton energy was increased from 75 to 115 keV.

The purpose of this paper is to extend the preliminary results of the x-ray yield measurements referred to above. Single crystals (fcc) of copper and aluminum were bombarded with protons of energy between 70 and 100 keV. The crystals were cut with the [001] direction normal to the surface. The [011] direction and a planar crossing of the (100) plane at 30° to the surface normal were studied in detail. Special care was taken to investigate the effect of surface imperfections, the presence of which was not fully studied in Ref. 10. The shapes of two arbitrarily chosen angular sweeps in the vicinity of the [011] direction were studied as a function of surface carbon contamination.

EXPERIMENTAL TECHNIQUE

A previous publication included a description of the general method of production of x rays by proton bombardment and the related apparatus employed in the present experiment.[11] Although the details will not be reproduced here, the experiment will be outlined to gain perspective.

The protons, supplied by a duoplasmatron ion source, are accelerated to energies up to 100 keV by a standard dc column of 10 dynodes. After magnetic analysis, to assure purity of ion component, and collimation, the protons are introduced into a separately (oil diffusion-) pumped target chamber. The target and the electron shield are both part of the current collecting system, which eliminates photoelectron currents. X rays produced in the target are observed at 90° to the proton beam. The detector for these soft x rays is a thin-window proportional counter (e.g., $\frac{1}{4}$-mil aluminized Mylar) operating in a reduced-pressure flow mode (20 cm Hg of 90% Ar+10% methane or 96% helium+4% isobutane, 10–30 cc/mm). The counter pulses are amplified and introduced into a charge-gated scaler after suitable differential discrimination and shaping. A pulse height analyzer is operated in coincidence with the scaler to assure drift-free measurements.

In channeling experiments care must be taken to assure proper collimation of the beam. Two $\frac{3}{16}$-in. collimators separated by 36 in. were employed, allowing

* Work performed under the auspices of the U. S. Atomic Energy Commission.

[1] G. R. Piercy, M. McCargo, F. Brown, and J. A. Davies, Can. J. Phys. **42**, 1116 (1964).
[2] J. A. Davies, G. C. Ball, F. Brown, and B. Domeij, Can. J. Phys. **42**, 1979 (1964).
[3] M. T. Robinson and O. S. Oen, Phys. Rev. **132**, 2385 (1963).
[4] L. Lehmann and G. Leibfried, J. Appl. Phys. **34**, 2821 (1963).
[5] A. L. Southern, W. R. Willis, and M. T. Robinson, J. Appl. Phys. **34**, 153 (1963).
[6] O. Almen and G. Bruce, Nucl. Instr. Methods **11**, 279 (1961).
[7] R. S. Nelson and M. W. Thompson, Phil. Mag. **8**, 1677 (1963).
[8] C. Erginsoy, H. E. Wigner, and W. M. Gibson, Phys. Rev. Letters **13**, 530 (1964).
[9] E. Bogh, J. A. Davies, and K. O. Nielsen, Phys. Letters **12**, 129 (1964).
[10] W. Brandt, J. M. Khan, D. L. Potter, R. D. Worley, and Harold P. Smith, Jr., Phys. Rev. Letters **14**, 42 (1965).
[11] J. M. Khan and D. L. Potter, Phys. Rev. **133**, A890 (1964).

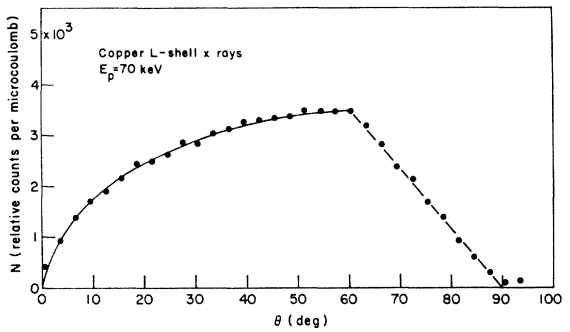

FIG. 1. Cu L-shell self-absorption normalization curve, counts versus tilt angle. The increase in counts from 0° to 60° reflects target self-absorption. The decrease from 60° to 90° reflects enlargement and displacement of the beam spot out of the detector's view. Beam energy (E_p) is 70 keV.

a maximum beam divergence of $\pm 0.3°$. This is about $\frac{1}{10}$ of the observed width and was considered acceptable.

The target holder allows two rotational degrees of freedom. The normal to the target surface may be tilted from 0° to 90° with respect to the proton beam. At any tilt angle (θ) the target may be rotated (ϕ) by 360°. Worm and bevel gear coupling is employed and refined to give reproducible readings to within $\pm\frac{1}{4}°$. By moving the controls in one direction better than $\frac{1}{10}°$ accuracy was obtained.

The proton beam intercepted the target surface at a distance from the center of rotation such that a 180° rotation of the target exposed a new portion of the surface to the beam. This allowed checks of the data to be made, thus assuring against unwanted contamination effects.

In making measurements at various tilt angles self-absorption of the soft x rays must be considered. To make the appropriate corrections, the single crystal was sanded with 600 grit abrasive, making the surface polycrystalline.[11] With the target in position the polycrystalline x-ray yield was measured from 0° to 90° tilt. The results of this measurement are shown in Fig. 1.

TARGET SURFACE

The condition of the surface of the target is of interest (a) before, (b) during, and (c) after bombardment. It will be a general conclusion of this paper that the low-energy channeling of protons is very strongly affected, if not dominated, by the surface state of the target. For this reason considerable space will be devoted to the authors' experience in contending with this problem.

(a) Before the crystal was subjected to bombardment it was necessary to prepare an "optimum" surface. It is believed that there are three surface properties of importance for channeling: physical smoothness, lattice structure, and chemical purity. Smoothness of the surface will affect the relative path lengths for the incident protons and the emitted soft x rays. The importance of obtaining a surface lattice structure reflecting the bulk, and a chemically pure surface, can be inferred from the data presented later. Imperfections in the vacuum-crystal interface, whether they are in the form of "contaminant" atoms or are geometrical in nature, can supply scattering centers which may alter the channeling process. The cleaning procedures described below were used to prepare the surfaces for the present measurements. The general electrolytic and chemical polishing techniques were based on those described in Ref. 12.

Copper. The surface was first rubbed lightly with Linde "C" alumina abrasive (Linde Company Crystal Products, Division of Union Carbide). This was followed by a chemical etch with a solution of 2 parts HNO_3, 1 part CH_3COOH, and 1 part H_3PO_4, applied to the crystal surface with an eye dropper. The crystal was subsequently electropolished in H_3PO_4, resulting in a smooth, highly reflective surface.

Aluminum. After a similar abrasive treatment the crystal was placed in a chemical etch solution (25 ml H_2SO_4, 70 ml H_3PO_4, 5 ml HNO_3) at 85°C for 5 min. The visual appearance of the surface was good, but the channeling data for aluminum suggests that this procedure may not be the best. (Electrolytic techniques were also tried but produced poorer results, indicated by low channeling ratios and the appearance of a surface film after bombardment.)

(b) During bombardment, carbon contamination and crystal imperfections may build up. It has been found in the past[13] that the carbon surface density for the currently employed target chamber may be described by the empirical relation

$$n=n_0+\beta(1-e^{-\alpha I_p})t,$$

where n is in units of atoms/cm², I_p in μA, and t in minutes. At 60 keV, $n_0=8\times10^{16}$, $\beta=0.7\times10^{16}$, $\alpha=0.35$. In the low-current approximation $n=n_0+\alpha\beta I_p t$, or the

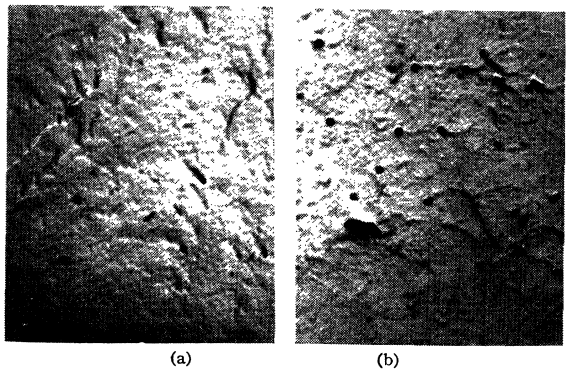

FIG. 2. Electron microscope photographs. (a) Unbombarded portion of Cu crystals; (b) increased "bubble" density in bombarded region.

[12] W. J. McG. Tegart, *The Electrolytic and Chemical Polishing of Metals* (Pergamon Press, Inc., New York, 1959).
[13] J. M. Khan, D. L. Potter, and R. D. Worley, Phys. Rev. **139**, A1735 (1965).

carbon atoms per charge or proton is a constant. Data will be presented as a function of surface contamination since x rays from the carbon atoms may be observed directly. The authors are not in a position to assay the effect of dislocations on the channeling data, as there was no control for the carbon contamination. It should be noted that the beam supplied only 7 mW of power to the crystal.

(c) After bombardment the crystal surface was markedly changed. The region of bombardment was generally stained in appearance, indicating carbon buildup. Another striking effect was observed when the chemical etch solution was applied (without abrasive cleaning). The unbombarded region of the crystal could be etched down by $\frac{1}{16}$ in. without any noticeable effect upon the stained region. It was necessary to remove the bombarded surface physically (10 sec with abrasive) to allow the etch to react uniformly. Electron-microscope analysis was employed to attempt to "see" this stained region. Figure 2 shows the results. The bombarded region (center of crystal) appears quite densely "bubbled." This photograph is of average bombarded effect, not selected to show the extreme.

CHANNELING OBSERVATIONS

Aluminum and copper (fcc) single crystals were obtained with the [001] direction normal to the face within $\pm 3°$. With such a crystal orientation it is possible to employ the appropriate stereographic projection (stereogram) to identify planes, directions, and their relative angular separations. The stereogram for the [001] direction normal to the crystal surface is shown in Fig. 3. The crystal-holder is designed to move the proton beam over the crystal with polar coordinates as independent variables in the stereogram in Fig. 3. A

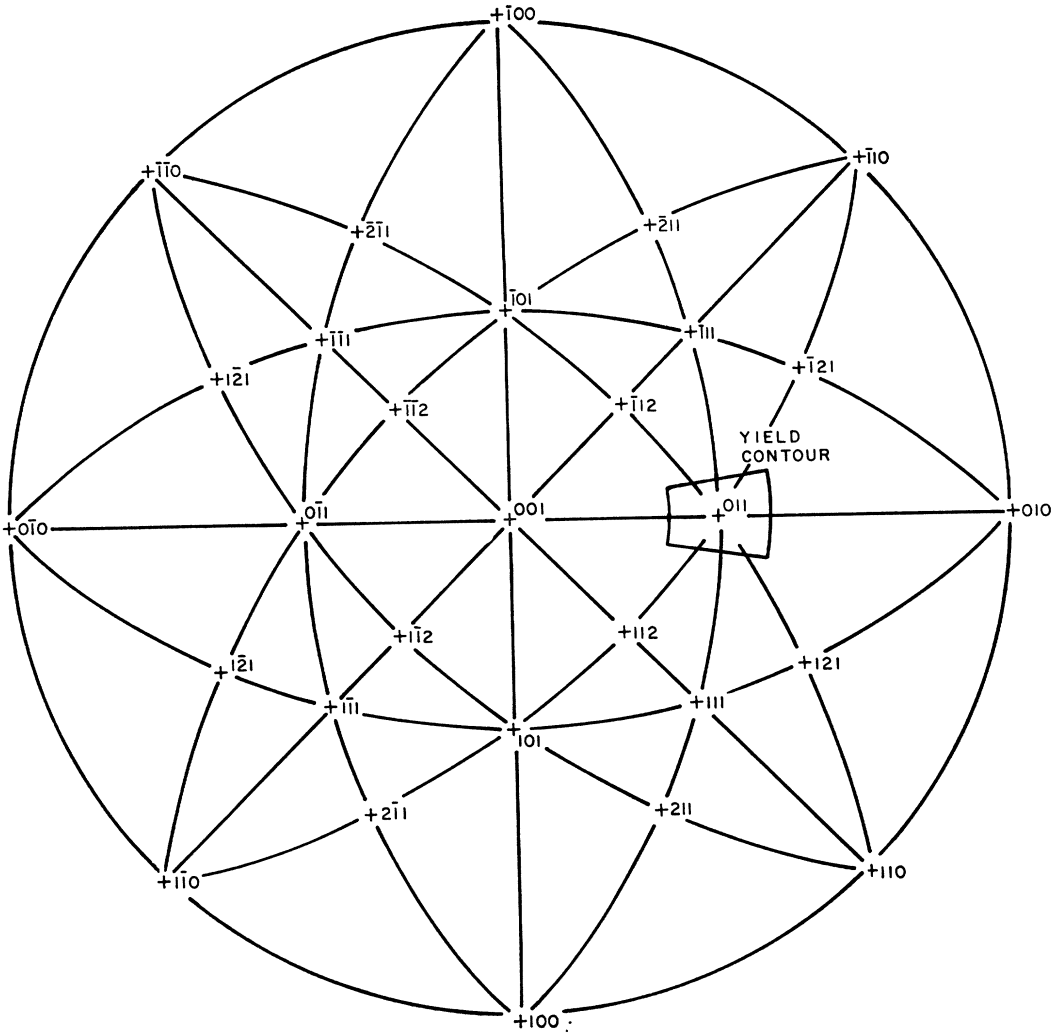

FIG. 3. [001] stereographic projection. The [001] direction is normal to the crystal surface. The yield contour (Fig. 5) location is shown at the [011] direction (45° to crystal surface).

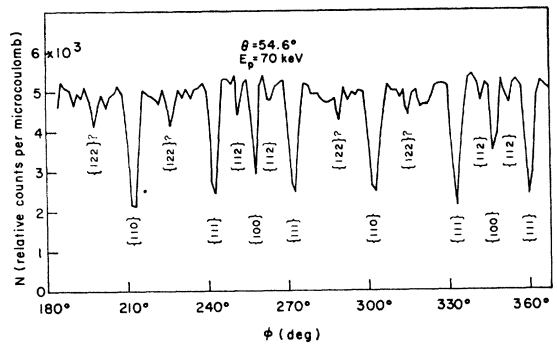

FIG. 4. ϕ sweep for copper at $\theta=54.6°$. $E_p=70$ keV.

constant tile angle (θ) will effectively constrain the beam to a circle on the stereogram whose center is the [001] direction, or (physically) to a cone centered about the normal to the crystal face. In the data presented below, three portions of the stereogram are chosen: (1) 180° sweep through ϕ at $\theta=54.6°$; (2) contour presentation (series of ϕ sweeps at different θ's) of the copper L-shell x-ray yield centered about a [011] direction at 45° to the surface normal (two sweeps from the contour are arbitrarily chosen as characteristic of the processes involved and are studied in detail); (3) to simplify the possible interpretations, a sweep across a (100) plane at $\theta=30°$ is shown for copper, since the [011] direction is the intersection of a number of planes.

Figure 4 illustrates the general sensitivity of x-ray production to the channeling of 70-keV protons for a ϕ sweep at $\theta=54.6°$ in copper. A number of identifiable planar crossing are observed. The largest effects are seen for (100), (110), and (111) planes, with many higher index planes appearing between them.

Figure 5 shows a contour of copper L-shell x-ray yield centered upon a [011] direction. The two dashed traces in the figure were chosen as interesting sweeps in the contamination study. These traces cross one (110) and two (111) planes as well as the [011] direction. The two starred points are locations of local maximum and minimum yield values. The ratio is 15; that is, *the x-ray yield has dropped to 6.7% of its maximum yield value*, where the lowest value corresponds to channeling along the [011] direction which is the intersection of one (100), one (110), two (111), and two (112) planes.

Figures 3, 4, and 5 give us a context in which we may place the more detailed studies. Three standard sweeps were chosen, two in the vicinity of the [011] direction and one crossing the (100) plane at 30° to the surface normal.

Surface Effects

Figure 6 shows the standard sweeps for aluminum and copper x-ray yields with various surface densities of carbon contamination.[13] The initial values for the carbon contamination (curve A) are the minimum values obtained in the present set of experiments.

The carbon x-ray yield was measured across the channel. There was no detectable channeling (changes were less than 3%), implying that the carbon was in an amorphous or polycrystalline state. The effect of contamination upon the copper and aluminum sweeps is dramatic. The yield value at the dip in the ϕ sweep at the [011] direction has increased, while the minimum in the θ sweep, where it crosses the $(0\bar{1}1)$ plane at the center of its scan, was almost obliterated for both elements.

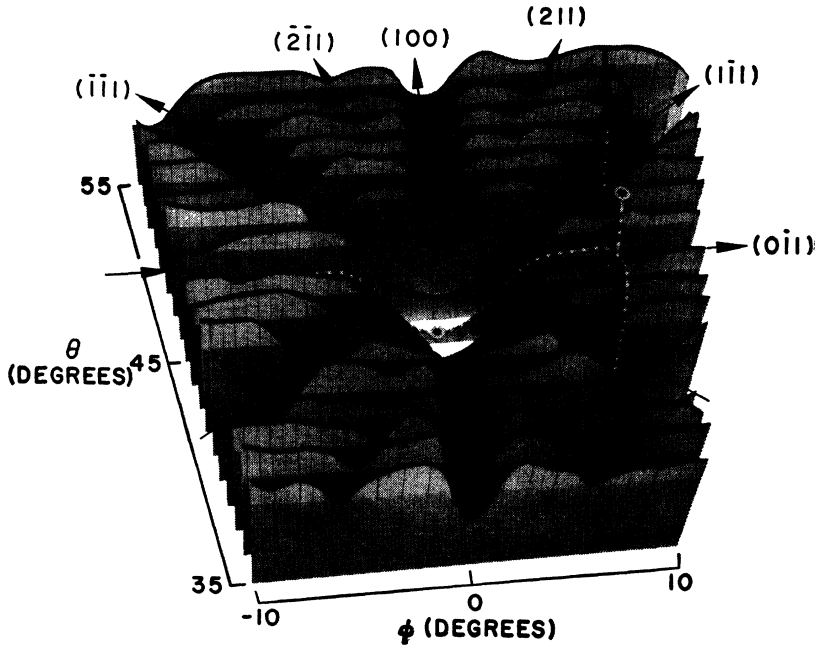

FIG. 5. Copper L-shell x-ray yield contour in the region of the [011] direction showing polycrystalline yield value (shaded area), intersecting planes, standard sweeps (dashed lines), and yield value extremes (starred points) whose ratio is 15. $E_p=70$ keV.

Energy Dependence

Figure 7 shows the change in shape with energy. The curves for aluminum were taken at 75 and 100 keV. The width of the ϕ sweep across the [011] direction changed by 16%. For copper that change was 25%, from 70 keV to 100 keV. Both decreased with increase in energy. Although the width change was small it is not inconsistent with an energy dependence of $E^{-1/2}$. Any stronger conclusion must wait for an expanded energy variation.

Single-Crystal versus Polycrystalline Yield

Referring again to Fig. 5, it is possible to see the large (30%) difference between single and polycrystalline yield values. The shaded area below the polycrystalline yield value clearly shows that much information is lost by the polycrystalline averaging of the yields. This casts some doubt upon the specific conclusions drawn from polycrystalline yield measurements when theoretical models for inner-shell ionization processes are tested. It would be highly instructive to compare these two yield measurements with the yield in the liquid state.

DISCUSSION

The observation of characteristic x rays produced in single crystals by positive-ion (proton) bombardment clearly shows an orientation dependence. The measurements also indicate that the surface condition is important in establishing the width and depth of the x-ray yield angular profiles, particularly at these low energies. "Channeling" along planes is observed as well as at the intersection of planes.

The sensitivity of the technique suggests that much may be learned of the interaction between positive ions and ordered arrays. The systematics involving Z, lattice geometry, atomic shells, and projectile have not yet emerged. In addition, the process of x-ray production should be re-evaluated. Factors that are implicit in this process are (1) the thick-target nature of the samples, (2) stopping power of the single crystals for protons of various channeled and unchanneled trajectories, (3) energy dependence of the x-ray production cross sections, and (4) self-absorption of the emitted x rays. (At low bombarding energies it is reasonable to assume that self-absorption of the x rays may be neglected.)

In the Appendix we employ the low-energy x-ray data and use a classical description of the proton in a static averaged potential to estimate the values of that potential and compare them with values proposed by Erginsoy.[14] The agreement is good except near the

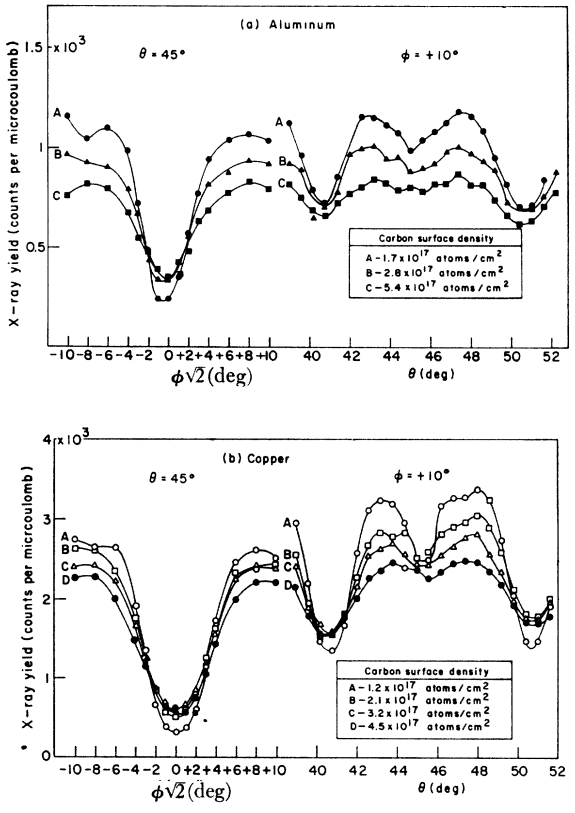

FIG. 6. Contamination effects in aluminum and copper at $E_p = 70$ keV. Standard sweeps (see Fig. 5) are shown.

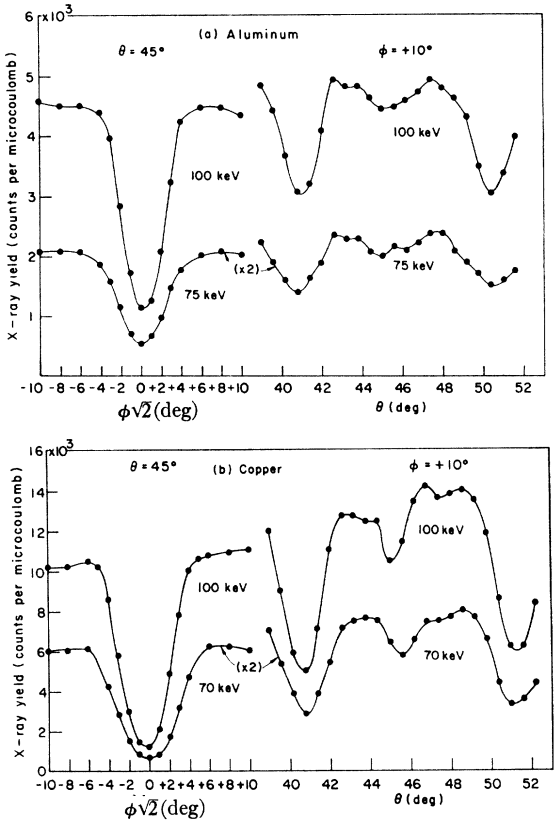

FIG. 7. Energy dependence of the shapes of the standard sweeps for (a) Al and (b) Cu.

[14] C. Erginsoy, Phys. Rev. Letters **15**, 360 (1965).

center of the channel. However, it is here that the model loses its validity.

ACKNOWLEDGMENTS

The authors would like to express their appreciation for the design and fabrication assistance rendered by Virgil Gregory, George Clough, and in particular William Fineren, III. To Marvin Williamson, whose many discussions regarding cleaning and surface preparation of high-purity crystals were most enlightening, we express special thanks.

APPENDIX: ESTIMATING THE PROTON-CRYSTAL POTENTIAL

We assume, as did Lindhard,[15] Erginsoy,[14] and Nelson and Thompson,[7] that the motion of a channeled proton can be closely approximated as a classical particle moving in a static conservative potential formed by suitably averaged arrays of scattering centers. In addition, experimental data, including that presented in this paper, suggest that channeling occurs primarily between low-index planes, and therefore the averaging process should be performed for planes. We would like to extend these considerations to estimate the averaged proton-crystal potential directly from x-ray yield data.

Conservation of energy in a direction perpendicular to the scattering planes requires, for the maximum displacement x of the channeled proton,

$$V(x)+E_p\alpha^2=V(X), \tag{1}$$

where x and X are distances from the center of the channel, E is the energy of the proton, and α is the incidence angle measured from the scattering plane. It is assumed that those protons having a maximum amplitude of oscillation less than X do not contribute in x-ray production. Since the protons impinge uniformly over the surface of the crystal, the relative x-ray yield may be defined by

$$y(\alpha)=1-2x(\alpha)/D, \tag{2}$$

where D is the planar spacing. The applicability of the model is restricted to small values of α, for which the proton energy transverse to the planar channel is small, thus eliminating the need for detailed consideration of proton-atom interactions. To include effects of beam divergence resulting from imperfect collimation, surface contamination, and radiation damage in the surface layers, Eq. (2) is rewritten as

$$y(\alpha)=1-\int_{-\pi/2}^{\pi/2} d\alpha' \frac{2x(\alpha')}{D} p(\alpha-\alpha'), \tag{3}$$

where $p(\alpha-\alpha')$ is the angular probability density function for the proton beam. In most channeling experiments, the beam divergence is small, and the following

[15] J. Lindhard, Phys. Letters 12, 126 (1964).

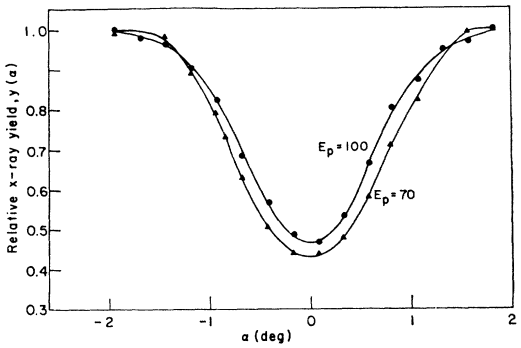

FIG. 8. Normalized experimental x-ray yield sweep across the (100) plane of copper at $\theta=30°$; $E_p=70$ and 100 keV.

approximate expressions may be used:

$$p(\alpha-\alpha')=1/2\delta \quad \text{for} \quad |\alpha-\alpha'|<\delta$$
$$=0 \quad \text{for} \quad |\alpha-\alpha'|>\delta,$$

and

$$x(\alpha')=x(\alpha)+(\alpha-\alpha')(dx(\alpha)/d\alpha)+\tfrac{1}{2}(\alpha-\alpha')^2[d^2x(\alpha)/d\alpha^2].$$

Substitution into Eq. (2) then yields

$$y(\alpha)=1-2x(\alpha)/D+\tfrac{1}{6}\delta^2 d^2y(\alpha)/d\alpha^2, \tag{4}$$

where it follows from Eqs. (2) and (3) that

$$d^2y(\alpha)/d\alpha^2\approx-(2/D)d^2x(\alpha)/d\alpha^2.$$

It should be noted that Eq. (4) is in agreement with the experimental results presented in Fig. 6 where increasing carbon contamination, which yields an increasing value of δ^2, has a maximum effect (with the proper sign) at those values of the yield where the curvature of the yield curve is greatest and practically no effect where the curvature is small. From Eqs. (1) and (4) and a value for δ, combined with measured values of $y(\alpha)$, D, and E_p, we can determine the averaged proton potential, $V(x)$.

Three inherent features may be noted: (a) The maximum amplitude X is determined by the minimum yield

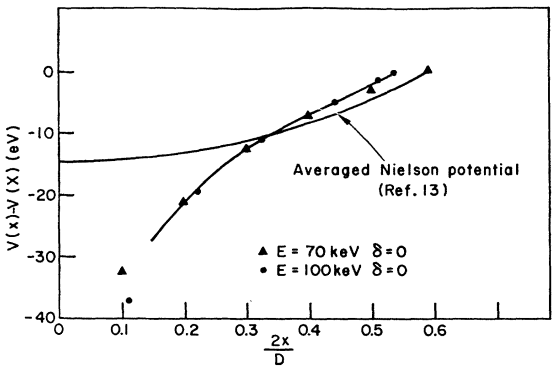

FIG. 9. Comparison of the calculated potential and the planar-averaged Nielsen potential of Ref. 13.

$y(0)$ under perfect collimation (i.e., $\delta=0$), and should not be a function of energy. (b) The calculated potential $V(x)$ should be independent of the proton energy, E_p. This requires that if (a) is satisfied, the angular width of $y(\alpha)$ should be inversely proportional to the square root of energy E_p. (c) Measurement of $y(\alpha)$ near $\alpha\approx 0$ produces values of $V(x)$ for $x\lesssim X$. However, values of $V(x)$ near $x=0$ are obtained for large α, where the model is not expected to be applicable. Consequently, the estimate of the potential near the center of the channel is not expected to be good.

The experiment was conducted with protons of energies 70 and 100 keV. The beam was swept across the (001) plane of a copper crystal for which the [001] direction was parallel to the surface normal. The plane was crossed at 30° to the surface normal and the stereogram of the (001) surface indicates that no other low-index planes were encountered during the sweep. The data are shown in Fig. 8.

The averaged potential was then calculated using the above equations. The results are shown in Fig. 9. For comparison, the planar-averaged Nielsen potential between two planes may be written

$$V(X)-V(x)=\frac{\pi Z_2 e^2 a_B}{A}K\ln\left[\frac{1-(4x^2/D^2)}{1-(4X^2/D^2)}\right],$$

where a_B is the atomic screening radius and $1/A$ is the atomic density in the plane.[14] This potential is also shown in Fig. 9, where good agreement appears between the calculated and the predicted potential for $x\lesssim X$ (i.e., for $\alpha\approx 0$).

PHYSICAL REVIEW VOLUME 148, NUMBER 1 5 AUGUST 1966

Wick's Theorem for Spin-½ Operators, with an Application to Spin Waves in Antiferromagnets*†

YUNG-LI WANG, S. SHTRIKMAN,‡ AND HERBERT CALLEN
Department of Physics, University of Pennsylvania, Philadelphia, Pennsylvania
(Received 20 December 1965)

An analog of Wick's theorem is developed for spin-½ operators, and a linked diagram expansion for spin Green's functions is derived. As an application we derive the familiar Anderson approximation for spin waves in antiferromagnets, and we then obtain the leading dynamical and kinematical corrections to that approximation. The Oguchi form of correction, usually obtained by a formal expansion in $1/S$ extrapolated to $S=\frac{1}{2}$, is found here as the leading term of an expansion in powers of $1/z$, where z is the number of nearest neighbors. However, the Oguchi result is here found to be valid only for spin waves with wavelengths greater than two or three interspin distances.

1. INTRODUCTION

A MAJOR difficulty in the theory of spin systems has been the lack of a practical analog of Wick's theorem. That theorem relates averages of products of many boson or fermion operators to averages of pairs, and it is the basis for the Feynman diagram representation of perturbation theory.[1] In this paper we develop such a theorem for spin operators, albeit of a somewhat more complicated form than in the fermion or boson cases, and we demonstrate the corresponding linked-diagram expansion.

As illustrations of the diagram method for spin operators, we first show that spin excitations in a ferromagnet generate diagrams which can be trivially summed to infinite order, giving the well-known rigorous spin-wave result.

The simplicity of the ferromagnetic case precludes a full demonstration of the diagrammatic method. To illustrate the more general aspects we then consider the nontrivial problem of spin excitations in a Heisenberg antiferromagnet. Summation of the lowest order (simple-chain) diagrams yields the familiar spin-wave approximation of Anderson.[2] We show that if we restrict our attention to spin waves with wavelengths greater than about two interspin distances, the diagrams can be classified according to their order in $1/z$, where z is the number of nearest neighbors. Furthermore this classification is equivalent to a classification according to the order in δS_0^z, the deviation from perfect alignment in the ground state. The leading diagrams in $1/z$ are chains dressed with bubbles (a dynamical correction) and with loops (a kinematical correction). The resultant correction reproduces the result of Oguchi.[3]

Although the excitation spectrum has been obtained

* Supported by the U. S. Office of Naval Research and the National Science Foundation.
† This work is a contribution of the Laboratory for Research on the Structure of Matter, University of Pennsylvania.
‡ Senior Foreign Scientist Fellow of the National Science Foundation. On leave from the Weizmann Institute of Science, Rehovoth, Israel.
[1] G. C. Wick, Phys. Rev. **80**, 268 (1950). For applications see, for example, S. Schweber, *An Introduction to Relativistic Quantum Field Theory* (Row, Peterson and Company, New York, 1962).
[2] P. W. Anderson, Phys. Rev. **86**, 694 (1952).
[3] T. Oguchi, Phys. Rev. **117**, 117 (1960).

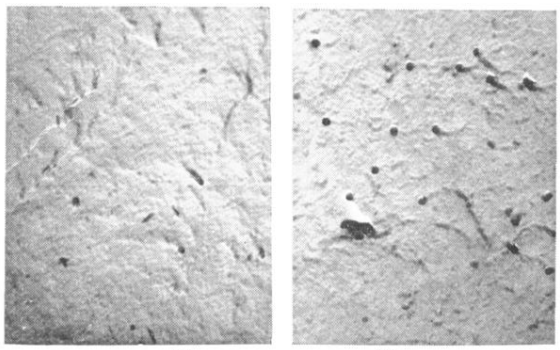

(a) (b)

FIG. 2. Electron microscope photographs. (a) Unbombarded portion of Cu crystals; (b) increased "bubble" density in bombarded region.

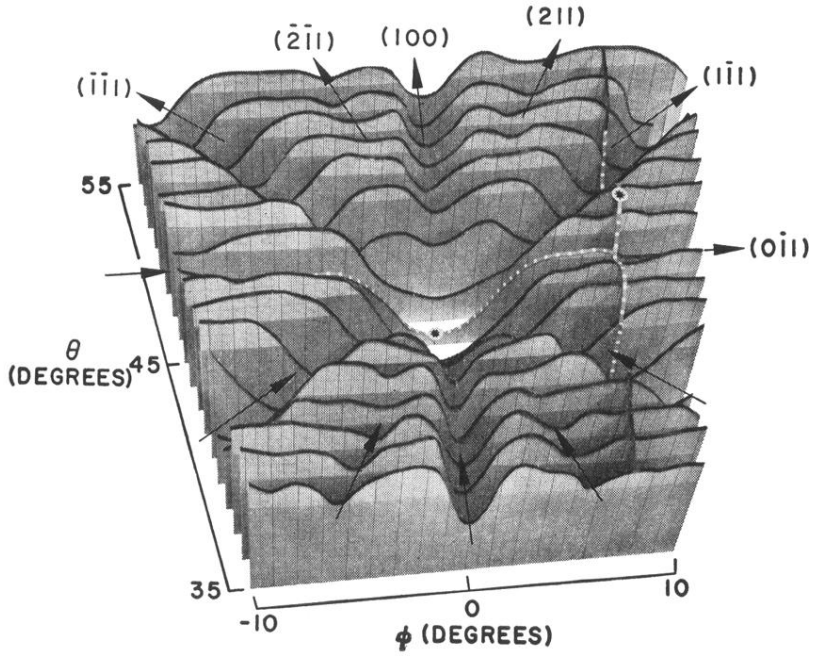

FIG. 5. Copper L-shell x-ray yield contour in the region of the [011] direction showing polycrystalline yield value (shaded area), intersecting planes, standard sweeps (dashed lines), and yield value extremes (starred points) whose ratio is 15. $E_p = 70$ keV.